Thin-Walled Structures 49 (2011) 1178–1183

Contents lists available at ScienceDirect

Thin-Walled Structures

journal homepage: www.elsevier.com/locate/tws

Shape functions of superconvergent finite element models

Hamid Ahmadian [a,*], Shirko Farughi [b]

[a] Center of Excellence in Experimental Solid Mechanics and Dynamics, School of Mechanical Engineering, Iran University of Science & Technology, Narmak, Tehran 16844, Iran
[b] School of Mechanical Engineering, Urmia University of Technology, Band Street, Urmia, Iran

ARTICLE INFO

Article history:
Received 24 December 2009
Received in revised form
19 April 2011
Accepted 16 May 2011

Keywords:
Finite element modeling
Trigonometric shape functions
Membrane element
Inverse method

ABSTRACT

In structural dynamics superconvergent element models are obtained by eigen-value convergence analysis, or minimizing the discretization errors leading to maximum convergence rates in their eigen-solutions. The element formulations developed by these inverse strategies are obtained in local coordinates. As no shape functions are employed in their development transforming them to global coordinates is a challenge and prevents their use in practical finite element models. To remove this obstacle a new method is proposed to obtain shape functions for superconvergent element models attained directly from the eigen-value convergence analysis or discretization error analysis. The method employs series of trigonometric functions to obtain shape functions corresponding to the superconvergent element formulations. Using the proposed strategy, the shape functions for super-convergent rod, beam and transverse vibration membrane are obtained. It is shown transformation of the superconvergent element formulation to the global coordinates using the obtained shape functions does not affect the eigen-value convergence rates.

1. Introduction

The accuracy of finite element (FE) models may be improved by number of methods. The first and most common method is H-version, in which the order of element is kept fixed while the number of elements is increased in a way that maximum size, h, of the elements approaches a small value [1]. The second method known as $\boldsymbol{p}$-version, whereby the mesh of the model is fixed and the order of the interpolation functions, $\boldsymbol{p}$, is progressively increased until meeting the desired degree of convergence [2]. Houmat [3,4] derived improved formulations for rod and transverse membrane elements using the later approach.

A rather different strategy in obtaining accurate FE models is to employ inverse methods. Considerable efforts in FE modeling have been devoted on obtaining an element formulation that gives a small discretization error and fast convergence. Employing inverse methods was firstly introduced by Argyris et al. [5], Bergan and Nygard [6] and Simo and Rafai [7] to enforce constraints on the stiffness formulation to guarantee the element model passing the patch test. MacNeal [8], Kim [9], Hanssan and Sandberg [10] and more recently Fried and Chavez [11] and Fried and Leong [12] obtained superconvergent models (SCM) by eigen-value convergence analysis for rod, beam and membrane elements in a local coordinate. Stavrinidis et al. [13] and Ahmadian et al. [14] derived superconvergent element formulations by minimizing the discretization errors for several elements in local coordinates. The drawback in these inverse approaches is that the element model is obtained in local coordinate system and as no shape function is employed in element model development, one is not capable to map the element model from local to global coordinates. This restricts the use of obtained models using inverse strategy in modeling practical structures.

To overcome this problem, Kim [9] proposed a method for obtaining shape functions of superconvergent rod element. He used a linear combination of shape functions associated with lumped and consistent mass matrices and adjusted the weighting for each function to achieve the superconvergent finite element model. In this method the diagonal components of mass matrix are always smaller than the diagonal components of the SCM obtained by an inverse approach, while the off-diagonal components are greater than those associated with SCM. SCM models of elements with rotational degrees of freedom such as beam [13] and bending plate elements cannot be established with a linear combination of lumped and consistent models. Therefore Kim's method cannot be used in these situations.

In this paper trigonometric series are used to establish the shape functions for SCMs. Trigonometric functions have been used as shape functions for vibration analysis of membranes [15] and Timoshenko beam element [16]. More recently, Shavezipur and Hashemi [17] used trigonometric shape function for analyzing non-uniform beams using refined dynamic finite element method. Christian [18] used trigonometric shape functions for investigating local buckling of stiffened composite plates.

The trigonometric series employed in the current paper to establish the shape functions for SCMs include some un-attributed

* Corresponding author.
E-mail address: ahmadian@iust.ac.ir (H. Ahmadian).

0263-8231/$ - see front matter © 2011 Elsevier Ltd. All rights reserved.
doi:10.1016/j.tws.2011.05.004

coefficients. These coefficients are set such that the obtained finite element model regenerates the SCM and also the corresponding shape functions satisfy the general requirements of compatibility, completeness, physically justifiable, etc. Using these shape functions, element model can be transformed from local to global coordinate systems. To demonstrate the efficiency of the method the shape functions for rod and transverse vibration membrane SCM are obtained using the proposed method. It is shown the eigen-value convergence rate remains the same when superconvergent element formulation is transformed to global coordinate using the obtained trigonometric shape functions.

The proposed approach specifies the shape functions of superconvergent eigen-value finite element models defined for linear systems with constant coefficient mass and stiffness matrices. As the nonlinearities in structures are usually due to stiffness or damping effects and the mass matrices of the model remain constant, the superconvergent mass models discussed in this paper can also be used in these problems to accurately represent the inertial forces of the model.

The rest of the paper runs as the following. In Section 2, the essential properties of shape functions are discussed. These properties are then enforced in development of shape functions for superconvegent element models. Sections 3 and 4 demonstrate the basic concept of developing trigonometric shape functions for SCMs of rod element and transverse vibration membrane element. Section 5 studies the performance of the mapped membrane element SCM using a numerical example, followed by the concluding remarks in Section 6.

2. Essential properties of shape functions

The quality of approximation achieved by Rayleigh–Ritz and FE approaches depends on the admissible assumed trial, field or shape functions. These functions can be chosen in many different ways. The most universally preferred method is the use of simple polynomials. It is also possible to use other functions such as trigonometric functions [15,18]. In general these functions must meet certain conditions. These conditions reported in references [19–21] are as follows:

1. Vertex modes have unit magnitude at one vertex and zero at all other vertices. A node (number i), with its coordinates represented by vector q_i, i.e. (x_i, y_i) or (x_i, y_i, z_i) for two or three dimensional elements, respectively, with shape function N_i possesses the following global Kronecker property:
$$N_i(q_j) = \delta_{ij} \Rightarrow \begin{cases} 1 & \text{for } i = j \\ 0 & \text{for } i \neq j \end{cases}. \quad (1)$$
2. Edges modes have magnitude along one edge and zero at all edges and vertices, i.e. vanishes over any element boundary (a side in 2D and a face in 3D) that does not include node i.
3. Inter-element compatibility and degrees of continuity (C^0, C^1,…).
4. Completeness condition.
5. Physical requirements that are imposed on shape functions, such as rigid body modes, element symmetry axes, etc.

The first four conditions are much explained in the literature. Moreover conditions 3 and 4 are consequences of the convergence requirements.

The physical requirements are related to the element geometry. The element has some rigid body modes. The selected shape functions must provide element deformed shapes compatible with the rigid body requirements. Also when the element has some symmetry axes the shape functions must represent these geometric properties. Consider two nodes of an element with geometric symmetry about an axis. By rotating the shape function associated with the first node about this axis the shape functions associated with the second node is obtained.

These essential requirements on the shape functions and the condition regarding their integral products produce the SCM that are imposed on trigonometric series to obtain the shape functions corresponding to the SCMs. The number of series terms is defined by the number of requirements that must be satisfied.

In the following the above requirements are enforced on truncated trigonometric series to obtain the shape functions of one- and two-dimensional rod and membrane elements.

3. Rod and beam elements with trigonometric shape functions

In this section, examples of rod and beam SCM are provided to demonstrate the procedures of determining their shape functions.

A two-node axial vibration rod element with length L, as shown in Fig. 1, is considered. Each node has one degree of freedom and the stiffness matrix, consistent and lumped mass matrices are

$$K = \frac{EA}{L}\begin{bmatrix} 1 & -1 \\ -1 & 1 \end{bmatrix}, \quad M_C = \frac{mL}{6}\begin{bmatrix} 2 & 1 \\ 1 & 2 \end{bmatrix}, \quad M_L = \frac{mL}{2}\begin{bmatrix} 1 & 0 \\ 0 & 1 \end{bmatrix}, \quad (2)$$

where m is the mass per unit length of the rod element, E is the module of elasticity and A is the cross section area. The eigen-convergence of rod element using lumped and consistent mass matrices is of the same order and their errors are of the order $O(L^4)$. McNeal [8] and Stavrinidis et al. [13] showed a SCM for rod element can be obtained by averaging of the lumped and consistent mass models:

$$M_{ave} = \frac{mL}{12}\begin{bmatrix} 5 & 1 \\ 1 & 5 \end{bmatrix}. \quad (3)$$

The averaged mass matrix produces eigen-solutions with the fourth order accuracy and the discretization errors are of the order $O(L^6)$ [13]. There is not any shape functions associated with the averaged mass matrix reported in the literature. One may use trigonometric functions to produce shape functions associated with the averaged mass matrix of Eq. (3). To obtain shape functions one should take the following steps.

The displacement field of the rod element is defined as

$$u(x) = N_1(x)u_1 + N_2(x)u_2. \quad (4)$$

where $N_1(x)$ and $N_2(x)$ are shape functions of rod element. Stavrinidis et al. [13] and Stavrinidis [22] considered the trigonometric shape functions $N_1 = \cos(\pi x/2L)^2$, and $N_2 = \sin(\pi x/2L)^2$ and obtained the mass matrix:

$$M = \frac{mL}{8}\begin{bmatrix} 3 & 1 \\ 1 & 3 \end{bmatrix}. \quad (5)$$

The resultant mass matrix produces a second order convergences rate in eigen-solutions. Following Stavrinidis et al. [13]

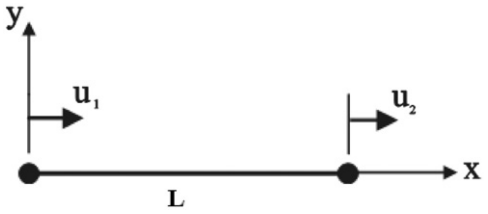

Fig. 1. Rod model element DOFs.

and Stavrinidis [22] we select the following trigonometric series for the shape function $N_1(x)$ associated with the non-consistent mass matrix of (3) as

$$N_1(x)=\sum_{n=1}^{N} a_n\cos\left(\frac{(2n-1)\pi x}{2L}\right)^2. \tag{6}$$

The shape function $N_2(x)$ is then readily available using rigid body requirement:

$$N_2(x)=1-N_1(x). \tag{7}$$

The selected series satisfies the first four conditions mentioned in Section 2 provided that

$$N_1(0)=\sum_{n=1}^{N} a_n=1. \tag{8}$$

The element has one symmetry axis and requires the following relations on the shape functions:

$$N_2(x)=N_1(L-x), \tag{9}$$

This leads to the requirement defined in Eq. (8), indicating the selected series reflects the physical properties of the element:

$$N_1(x)+N_1(L-x)=1,$$
$$\Rightarrow \sum_{n=1}^{N} a_n\left(\cos\left(\frac{(2n-1)\pi x}{2L}\right)^2+\cos\left(\frac{(2n-1)\pi(L-x)}{2L}\right)^2\right)=\sum_{n=1}^{N} a_n=1. \tag{10}$$

The shape functions $N_1(x)$ and $N_2(x)$ are required to produce the superconvergent mass matrix of (3), i.e.

$$\int_0^L N_1^2(x)dx=\int_0^L N_2^2(x)dx=\frac{5}{12},\quad \int_0^L N_1(x)N_2(x)dx=\frac{1}{12}. \tag{11}$$

The identities of (11) add only one more quadratic equation that brings the total number of equations regarding the coefficients of the series defined in Eq. (6) into two. There are two equations to be satisfied and it is decided to set $N=2$. The series coefficients of the trigonometric function of (6) are obtained as $a_1=1/2+\sqrt{15}/6$ and $a_2=1/2-\sqrt{15}/6$ leading to

$$N_1(x)=\left(\frac{1}{2}+\frac{\sqrt{15}}{6}\right)\cos\left(\frac{\pi x}{2L}\right)^2+\left(\frac{1}{2}-\frac{\sqrt{15}}{6}\right)\cos\left(\frac{3\pi x}{2L}\right)^2. \tag{12}$$

The resulting shape functions are shown in Fig. 2. The rod SCM element is derived using these shape functions, a task which was not successful by combination of consistent and lumped shape functions [9].

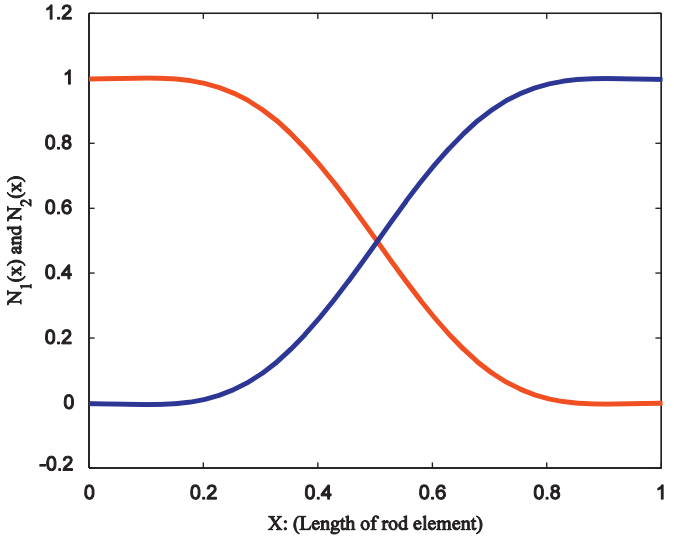

Fig. 2. The shape functions of rod element ($N_1(x)$—red, $N_2(x)$—blue). (For interpretation of the references to color in this figure legend, the reader is referred to the web version of this article.)

A similar procedure as in the case of rod element is followed to obtain associated C1 continuity shape functions of a superconvergent beam element. Stavrinidis et al. [13] derived a superconvergent model for the Euler–Bernoulli beam element using an inverse approach as

$$K=\frac{1}{dx^3}\begin{bmatrix} 12 & 6 & -12 & 6\\ & 4 & -6 & 2\\ & & 12 & -6\\ sym & & & 4\end{bmatrix},\quad M=\frac{dx}{840}\begin{bmatrix} 326 & -51 & 94 & 19\\ & 15 & -19 & -6\\ & & 326 & 51\\ sym & & & 15\end{bmatrix}. \tag{13}$$

Trigonometric series for the shape functions $N_k(\zeta)$, $k=1,2,3,4$ associated with the non-consistent mass matrix of (13) are selected based on Beslin and Nicolas proposal [26] as

$$N_k(\zeta)=\sum_{r=1}^{N} e_{k,r}\sin(2a_r\zeta+2b_r)\sin(2c_r\zeta+2d_r),\quad r=1,2,3,\ldots \tag{14}$$

The coefficients of these hierarchical functions a_r, b_r, c_r and d_r are tabulated in Table 1. The first four terms satisfy beam classical boundary conditions and higher order terms are used to improve the element convergence properties. These higher order terms have zero nodal displacements and slopes.

The shape function $N_1(\zeta)$ is unity at $\zeta=0$ and zero at $\zeta=1$ with zero slopes at these nodes. These boundary conditions are satisfied by including the term $r=1$ in the series defined in (14). The shape function $N_1(\zeta)$, apart from a constant shift, is anti-symmetric with respect to the beam symmetry axis and this property is reflected in the associated series by selecting even orders of $r>4$, i.e.

$$N_1(\zeta)=e_{1,1}\cos^2(\pi\zeta/2)-e_{1,6}\sin(2\pi\zeta)\sin(\pi\zeta)-e_{1,8}\sin(4\pi\zeta)\sin(\pi\zeta)+\cdots \tag{15}$$

The symmetry of the element enables one to define $N_3(\zeta)$ by rotating function $N_1(\zeta)$ about the symmetry axis as

$$N_3(\zeta)=N_1(1-\zeta). \tag{16}$$

The requirement (16) results

$$N_3(\zeta)=e_{1,1}\sin^2(\pi\zeta/2)+e_{1,6}\sin(2\pi\zeta)\sin(\pi\zeta)+e_{1,8}\sin(4\pi\zeta)\sin(\pi\zeta)+\cdots \tag{17}$$

Similarly the shape function $N_k(\zeta)$, $k=2,4$ can be composed of trigonometric hierarchical functions (14) as

$$N_2(\zeta)=e_{2,2}\sin(\pi\zeta)\cos(\pi\zeta/2)+e_{2,5}\sin^2(\pi\zeta)+e_{2,6}\sin(\pi\zeta)\sin(3\pi\zeta)+e_{2,7}\sin(\pi\zeta)\sin(2\pi\zeta)+e_{2,8}\sin(\pi\zeta)\sin(4\pi\zeta)+\cdots \tag{18}$$

The shape function $N_2(\zeta)$ contains the series term $r=2$ to satisfy the related boundary conditions, and all orders of $r>4$ as this function is neither symmetric nor anti-symmetric with respect to the beam symmetry axis. The shape functions $N_k(\zeta)$, $k=2,4$ must represent the symmetry properties of element, i.e.

$$N_4(\zeta)=-N_2(1-\zeta). \tag{19}$$

Table 1
The trigonometric series coefficients [27].

r	a_r	b_r	c_r	d_r
1	$\frac{\pi}{4}$	$\frac{3\pi}{4}$	$\frac{\pi}{4}$	$\frac{3\pi}{4}$
2	$\frac{\pi}{4}$	$\frac{3\pi}{4}$	$-\frac{\pi}{2}$	$-\frac{3\pi}{2}$
3	$\frac{\pi}{4}$	$-\frac{3\pi}{4}$	$\frac{\pi}{4}$	$-\frac{3\pi}{4}$
4	$\frac{\pi}{4}$	$-\frac{3\pi}{4}$	$\frac{\pi}{2}$	$-\frac{3\pi}{2}$
$r>4$	$\frac{\pi}{2}(r-4)$	$\frac{\pi}{2}(r-4)$	$\frac{\pi}{2}$	$\frac{\pi}{2}$

This leads to

$$N_4(\zeta) = -e_{2,2}\sin(\pi\zeta)\sin(\pi\zeta/2) - e_{2,5}\sin^2(\pi\zeta) - e_{2,6}\sin(\pi\zeta)\sin(3\pi\zeta) + e_{2,7}\sin(\pi\zeta)\sin(2\pi\zeta) + e_{2,8}\sin(\pi\zeta)\sin(4\pi\zeta) + \cdots \quad (20)$$

The unknown coefficients of shape functions $N_k(\zeta)$, $k=1,\ldots,4$ can be determined from further requirements that they must reproduce the superconvergent mass matrix of (13)

$$M_{ij} = \int_0^1 N_i(\zeta)\, N_j(\zeta) d\zeta. \quad (21)$$

These coefficients are obtained up to $r=8$ using requirements (21) as

$$e_{1,1}=1, \quad e_{1,6}=0.003, \quad e_{1,8}=-0.221, \quad e_{2,2}=0.318,$$
$$e_{2,5}=-0.104, \quad e_{2,6}=-0.100, \quad e_{2,7}=0.032, \quad e_{2,8}=-0.138. \quad (22)$$

The element has two rigid body modes and the defined shape functions produce these modes:

$$N_1(\zeta)+N_3(\zeta)=1,$$
$$\frac{N_3(\zeta)-N_1(\zeta)}{2}+N_2(\zeta)+N_4(\zeta)=\zeta-\frac{1}{2}. \quad (23)$$

Similarly shape functions of other C1 element types such as bending plate elements can be obtained using these trigonometric hierarchical functions as defined in Ref. [26].

The rod and beam examples demonstrate the important steps in obtaining the shape functions of a SCM. The same steps will be followed in the next section to construct trigonometric shape functions for SCM of a transverse vibrating membrane element.

4. Four-nodes square membrane element

A membrane is characterized by dominating tension and a negligible resistance for bending [23]. The membrane vibration problem as the simplest two-dimensional problem is considered by number of researchers [11,12,24], and is used to verify the performance of numerical techniques [3].

In this paper, a four-node square transverse vibrating membrane element of side length dx as shown in Fig. 3 is considered. The element has one out-of plane degree of freedom at each node. The normalized stiffness matrix for transverse vibrating square membrane element and its consistent and lumped mass matrices developed using bilinear shape functions are [25]

$$K=\frac{1}{6}\begin{bmatrix} 4 & -1 & -2 & -1 \\ & 4 & -1 & -2 \\ & & 4 & -1 \\ sym & & & 4 \end{bmatrix}, \quad M_C=\frac{dx^2}{9}\begin{bmatrix} 4 & 2 & 1 & 2 \\ & 4 & 2 & 1 \\ & & 4 & 2 \\ sym & & & 4 \end{bmatrix},$$
$$M_L=\frac{dx^2}{9}\begin{bmatrix} 1 & 0 & 0 & 0 \\ & 1 & 0 & 0 \\ & & 1 & 0 \\ sym & & & 1 \end{bmatrix}. \quad (24)$$

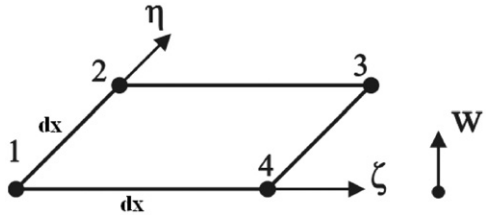

Fig. 3. Four-node square transverse vibrating membrane element.

The eigen-problems formed using consistent and lumped mass matrices produce second order convergence rates in eigen-solutions while the weighted averaged of lumped and consistent mass matrix leads to a fourth order eigen solution convergence rate [11]:

$$M_{ave}=\frac{dx^2}{48}\begin{bmatrix} 7 & 2 & 1 & 2 \\ & 7 & 2 & 1 \\ & & 7 & 2 \\ sym & & & 7 \end{bmatrix}. \quad (25)$$

No shape functions associated with this mass matrix are reported in the literature. This paper employs two-dimensional trigonometric functions to obtain shape functions corresponding to the superconvergent mass model. The steps followed to obtain shape functions of membrane SCM are the same as those of rod SCM. First, the displacement field of the element is defined:

$$w(\zeta,\eta)=N_1(\zeta,\eta)w_1+N_2(\zeta,\eta)w_2+N_3(\zeta,\eta)w_3+N_4(\zeta,\eta)w_4, \quad (26)$$

where ζ and η are natural coordinates of the elements $\zeta=x/dx$ $\eta=y/dx$ as shown in Fig. 3. The element has one rigid body mode, which establishes the following requirement on the shape functions of the membrane element:

$$N_4(\zeta,\eta)=1-N_1(\zeta,\eta)-N_2(\zeta,\eta)-N_3(\zeta,\eta). \quad (27)$$

The shape functions are expressed as linear combinations of the trigonometric functions as

$$N_1(\zeta,\eta)=\sum_{n=1}^{N}\sum_{m=1}^{N} a_{nm}\cos\left(\frac{(2m-1)\pi\zeta}{2}\right)^2\cos\left(\frac{(2n-1)\pi\eta}{2}\right)^2,$$
$$N_2(\zeta,\eta)=\sum_{n=1}^{N}\sum_{m=1}^{N} a_{nm}\cos\left(\frac{(2m-1)\pi\zeta}{2}\right)^2\sin\left(\frac{(2n-1)\pi\eta}{2}\right)^2,$$
$$N_3(\zeta,\eta)=\sum_{n=1}^{N}\sum_{m=1}^{N} a_{nm}\sin\left(\frac{(2m-1)\pi\zeta}{2}\right)^2\sin\left(\frac{(2n-1)\pi\eta}{2}\right)^2. \quad (28)$$

The element has two symmetry axes and an applied displacement at one node while the other nodes are fixed, apart from a constant, produces an anti-symmetric deformation $w(\zeta,\eta)$ with respect to the element coordinates. The selected form for the shape functions in Eq. (28) reflects this fact. Also the produced deformations along both element deformed edges are the same and therefore the numbers of series terms in both directions are kept the same. Changing the unit displacement practice from one node to the neighboring one the deformation field of the element is rotated by $\pi/2$ about axes normal to the element plane. This property is also regarded in the functions introduced in Eq. (28). Stavrinidis et al. [13] used the first term of these series to obtain mass matrix of rectangular in-plane element.

There are two more requirements that must be satisfied by series defined in Eq. (28) leading to specifications of series coefficients a_{nm}. They are

1. The function $N_i(\zeta,\eta)$, $i=1,2,3$, must be unity at node i and zero at other nodes, i.e.

$$\sum_{n=1}^{N}\sum_{m=1}^{N} a_{nm}=1. \quad (29)$$

This requirement produces a linear relation between the series coefficients.

2. These functions must produce the entries of membrane SCM defined in Eq. (14):

$$\iint_A N_i(\zeta,\eta)N_j(\zeta,\eta)dA=m_{ij}. \quad (30)$$

The requirements defined in Eqs. (29) and (30) produce four independent equations to be satisfied and therefore N is set equal

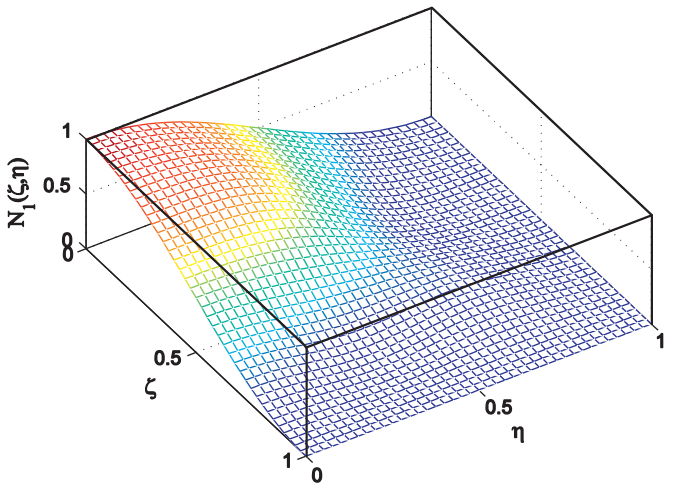

Fig. 4. Shape function $N_1(\zeta,\eta)$ of transverse vibrating membrane element.

to 2. The series coefficients of shape functions $N_i(\zeta,\eta)$, $i=1,2,3$, are obtained as

$$\begin{matrix} a_{11}=1+\beta, \\ a_{12}=a_{21}=-\beta, \quad \beta=\frac{551}{4178}. \\ a_{22}=\beta, \end{matrix} \tag{31}$$

The obtained trigonometric shape function $N_1(\zeta,\eta)$ of square membrane SCM is shown in Fig. 4. The other three shape functions are obtained by rotation of $N_1(\zeta,\eta)$ about the axis normal to the element plane.

The newly obtained shape functions are employed to transform element formulation from local to global coordinate systems and use the superconvergence property of the model in global coordinate. The element displacement field is transformed using the trigonometric shape functions whereas the geometry of element is mapped by employing bilinear shape functions.

Numerical performance of the model obtained using the new shape functions for transverse vibrating membrane element and its convergence rate in estimating the membrane eigen-values are demonstrated in the next section.

5. Numerical example

A simply supported sectorial membrane with $a/b=0.5$ and $\phi=90^\circ$ as shown in Fig. 5 is considered. The fundamental frequency parameter for such a sectorial membrane is $\Omega_{11}=6.8138$ [24]. The sectorial membrane is analyzed by transforming the square elements into quadrilateral elements as shown in Fig. 6. The consistent model, the model proposed by Hansson and Sandberg [10], obtained by linear combination of lumped and consistent element shape functions and membrane SCM, is mapped into global coordinate. The element geometry and displacements are mapped by bilinear shape functions for the consistent model while in cases of models proposed in [10] and membrane SCM the element geometry is mapped by bilinear shape function and the displacement fields are mapped by each model's respective shape function. The stiffness model, given in Eq. (24), is mapped using the bilinear shape functions in all models.

In order to investigate the convergence rate of solutions estimated by various membrane element models, the eigen-predictions obtained by the model proposed in [10], the consistent model and membrane SCM are shown in Figs. 7–9 for the sectorial membrane with different number of meshes. Figs. 7–9 show the error in the computed natural frequencies of the sectorial membrane versus the number of radial elements on

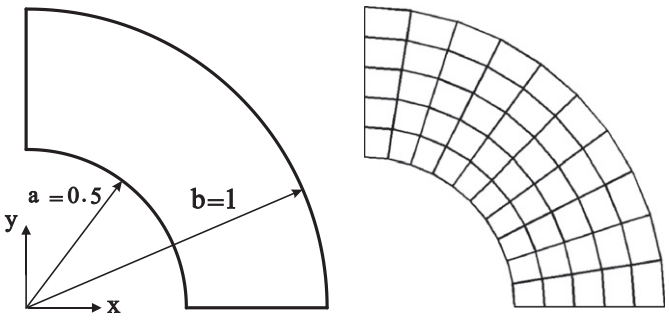

Fig. 5. The open sectorial membrane and its finite elements mesh.

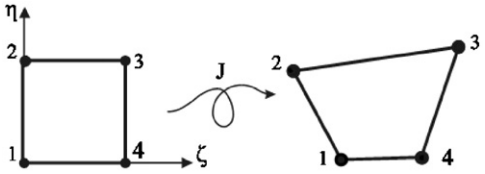

Fig. 6. Two-dimensional 'mapping' of the square element.

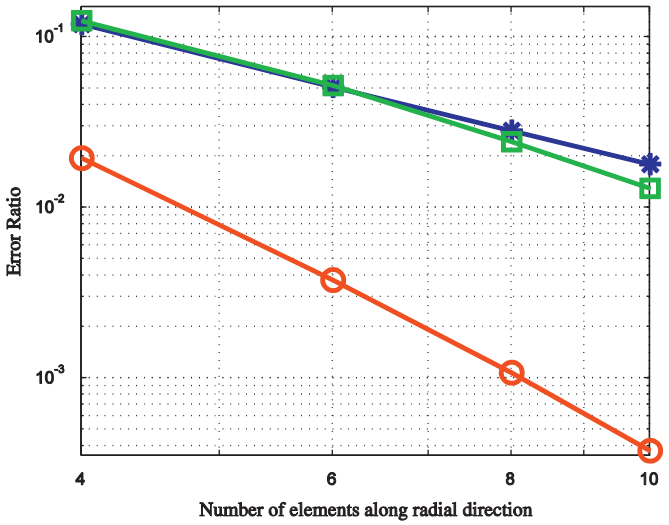

Fig. 7. Error in estimation of fundamental eigenvalue of the clamped membrane (SCM—○, Consistent model—*, Combinative model—□ [10]).

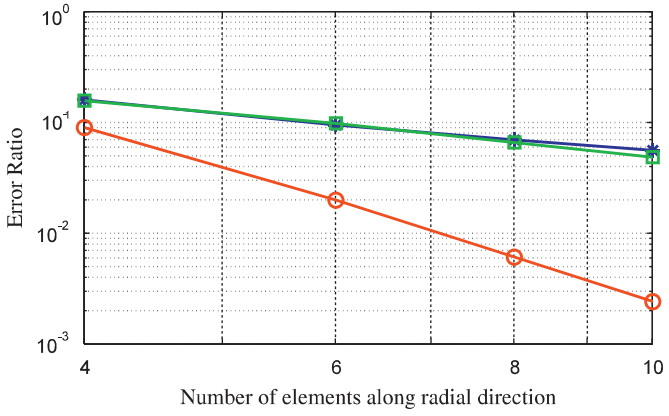

Fig. 8. Error in estimation of second eigenvalue of the clamped membrane (SCM—○, Consistent model—*, Combinative model—□ [10]).

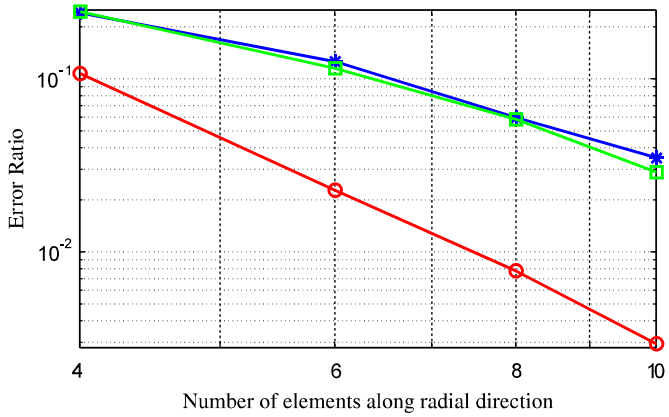

Fig. 9. Error in estimation of third eigenvalue of the clamped membrane (SCM—○, Consistent model—*, Combinative model—□ [10]).

Table 2
The fundamental eigenvalue of membrane obtained using the SCM.

N	4 point Gauss quadrature	9 point Gauss quadrature
4	6.680669213	6.680669213
6	6.788071811	6.788071812
8	6.806441098	6.806441099
10	6.811234720	6.811234721

logarithm scale. The number of meshes in radial direction is twice as that in angular direction. In this example the convergence rate of mapped membrane SCM is of order four while the consistent and the combinative [10] formulations produce convergence rate of the order two in estimating the first three eigen-values.

In deriving the membrane element formulation in local coordinates no numerical integration procedure is employed and the model is obtained analytically. However in transforming the element mass matrix from local to global coordinates, displacement fields are mapped by the respective shape functions and the integrals are performed based on Gauss–Legendre quadrature rule.

As shown in reference [27] the order of Gauss quadrature in the mass formulation has negligible influence on the lower eigenvalues. And substantial saving in computation time is achieved when a low-order Gauss quadrature is used for the evaluation of the mass matrix. To verify this influence the mass matrix of membrane numerical example in Section 5 is evaluated using 4 and 9 Gauss points. The fundamental eigenvalue obtained from these two mass matrices for different number of elements along radial sides ($N=4, 6, 8, 10$) is shown in Table 2. It can be seen there are no significant differences between the two sets of results.

6. Conclusion

Trigonometric functions are employed to define shape functions of SCM obtained by eigen-value convergence analysis, or minimizing the discretization errors. These trigonometric shape functions are then used to transform the displacement field of element under consideration to the global coordinates. The improvements in estimating the eigen-value using trigonometric shape functions in global coordinate are demonstrated using an example of sectorial transverse vibrating membrane. It is shown the accuracy of SCM is kept unchanged in global coordinates and higher order of accuracy is achieved compared to the common formulations existing in the literature.

References

[1] Zienkiwicz OC, Taylor RL. The finite element method. vol 1, 4th edition, New York: McGraw-Hill; 1989.
[2] Houmat A. A sector elliptic p-element applied to membrane vibrations. Thin-Walled Structures 2009;47:172–7.
[3] Houmat A. Free vibration analysis of arbitrarily shaped membranes using the trigonometric p-version of the finite element method. Thin-Walled Structures 2006;44:943–51.
[4] Houmat A. A sector Fourier p-element for free vibration analysis of sectorial membranes. Computer & Structures 2001;79:1147–52.
[5] Argyris JH, Hasse M, Mlejnek HP. On an unconventional but natural formulation of stiffness matrix. Computer Methods in Applied Mechanics and Engineering 1980;22:1–22.
[6] Bergan PG, Nygard MK. Finite element with increased freedom in choosing shape function matrix. International Journal for Numerical Methods in Engineering 1984;20:643–63.
[7] Simo C, Rifai MS. A class of mixed assumed strain methods and the method of incompatible modes. International Journal for Numerical Methods in Engineering 1990;29:1595–638.
[8] MacNeal—Schwendler Crop. NASTRAN Theoretical Manual. Los Angeles, CA; 1972.
[9] Kim KI. A review of mass matrices for eigenproblems. Computers & Structure 1993;46:1041–8.
[10] Per-Anders Hansson, Goran Sandberg. Mass matrices by minimization of modal errors. International Journal for Numerical Methods in Engineering 1997;40:4259–71.
[11] Fried I, Chavez M. Superaccurate finite element eigenvalue computation. Journal of Sound and Vibration 2004;275:415–22.
[12] Isaac Fried, Kaiwen Leong. Super accurate finite element eigenvalue via a Rayleigh quotient correction. Journal of Sound and Vibration 2005;288:375–86.
[13] Stavrindis C, Clinckemailliet J, Dubois J. New concepts for finite element mass matrix formulations. AIAA Journal 1989;27:1249–55.
[14] Ahmadian H, Friswell MI, Mottershead JE. Minimization of the discretization error in mass and stiffness formulation by inverse method. International Journal for Numerical Methods in Engineering 1998:371–87.
[15] Milsted MG, Hutchinson JR. Use of trigonometric terms in the finite element method with application to vibration membranes. Journal of Sound and Vibration 1974;32:327–46.
[16] Heppler GR, Hansen JS. Timoshenko beam finite elements using trigonometric basis functions. AIAA Journal 1988;11:1378–86.
[17] Shavezipur M, Hashemi SM. Free vibration of triply coupled centrifugally stiffened non-uniform beams using a refined dynamic finite element method. Aerospace Science and Technology 2009;13:59–70.
[18] Christian M. Explicit local buckling analysis of stiffened composite plates accounting for periodic boundary conditions and stiffener–plate interaction. Composite Structures 2009;91:249–65.
[19] Hutton DV. Fundamentals of finite element analysis. McGraw Hill; 2004.
[20] Rao SS. The finite element method in engineering. Elsevier Science & Technology Books; 2004.
[21] Felippa C. Introduction to finite element methods. http://www.colorado.edu/engineering/CAS/courses.d/IFEM.d/Home.htme;2009.
[22] Stavrinidis C. Dynamic flight load charts for spacecraft design. In: Proceedings of the AIAA/ASME/ASCE/AHS 22nd structures structural dynamics and materials conference, AIAA, New York, April, 280–5; 1981.
[23] Rao S. Vibration of continues system. John Wiley & Sons; 2007.
[24] Houmat A. Hierarchical finite element analysis of the vibration of membranes. Journal of Sound and Vibration 1997;201:465–72.
[25] Kwon Y, Bang H. The finite element method using Matlab. 2nd edition. Boca Raton, FL: CRC Press; 2000.
[26] Beslin O, Nicolas J. A hierarchical functions set for predicting very high order plate bending modes with any boundary conditions. Journal of Sound and Vibration 1997;202(5):633–55.
[27] Aggarwala KR, Sinhasanb R, Groverb GK. The effect of the order of Gauss quadrature on the free vibrations of plates in fluid. Applied Mathematical Modeling 38, 1980;4(6):433–4.